

# Surface plasmon resonance sensor based on photonic crystal fiber filled with silver nanowires

XIANGYONG FU, YING LU\*, XIAOHUI HUANG, CONGJING HAO, BAOQUN WU, JIANQUAN YAO

College of Precision Instrument and Opto-Electronics Engineering, Tianjin University, Tianjin 300072, P.R. China,

Key Laboratory of Opto-Electronics Information Technology (Tianjin University), Ministry of Education, Tianjin 300072, P.R. China

\*Corresponding author: luying@tju.edu.cn

Silver nanowire filled photonic crystal fibers are proposed in this paper to achieve surface plasmon resonance sensors and overcome the complicity and difficulty of coating the holes in the photonic crystal fiber. Optical field distributions of these fibers at different wavelengths are calculated and simulated using the finite element method (FEM), and the sensing properties are discussed in both areas of resonant wavelength and intensity detection. Numerical simulation results show that carefully designed structure of the sensor brings about an excellent effect, with both spectral and intensity sensitivity in the range of  $4 \times 10^{-5}$ – $5 \times 10^{-5}$  RIU, better than in the case of similar structures coated with metal film, and the fabrication is expected to be simplified.

Keywords: surface plasmon resonance, photonic crystal fiber, silver nanowire, sensor.

## 1. Introduction

The detection and analysis of biological materials are widely needed in many important areas in production and daily life, such as medicine, environment, biotechnology, food, *etc.* Surface plasmon resonance-based biochemical sensing method is currently the most advanced real-time and label-free detection technology.

Surface plasmon resonance (SPR) refers to the excitation of surface plasmon polaritons (SPPs), which are electromagnetic waves coupled with free electron density oscillations on the surface between a metal and a dielectric medium (or air) [1]. SPPs or surface plasmon waves (SPWs) are TM polarized electromagnetic waves and propagate along the interface of metal and dielectric materials with electromagnetic field decaying exponentially in both the metal and dielectric [2].

Surface plasmons can be excited by light as the phase matching condition between the exciting light and the surface plasmons is met. Commonly employed methods for surface plasmon excitation primarily use prism coupling, planar waveguide coupling, fiber optic coupling, and grating coupling method. The prism light coupling method is among the earliest techniques, including the Otto [3] and Kretschmann–Reather configuration [4, 5]. Plasmon resonance depends on the refractive index in the vicinity of the metal film within 100 nm. When the resonance occurs, most energy of the exciting light is absorbed by the surface plasmons, resulting in a sharp decrease in intensity of incident light. The detection of biological materials bound to the metal film using this method has unprecedented high sensitivity [6]. Progress of biological response can be obtained by detecting the angle [6, 7], spectral [8] and phase [9, 10] characteristics of the reflected light. For several decades of development, there have been many practical products available used in detection of biochemical substances. However, large size and high cost greatly limit the application range of the prism-coupling configuration.

With the rapid development of optical fiber manufacturing process, the need of miniaturization and integration in sensors promotes the research and development of the fiber coupled plasmon resonance sensors, and many compact fiber-optic SPR sensors have been studied, such as the metal film coated single-mode fiber, multi-mode fiber, polarization maintaining fiber, tapered fiber, Bragg grating, *etc.* [11–19]. Although the use of optical fibers provides an attractive platform for the SPR sensing, removing part cladding of the single-mode fiber by physical or chemical methods is often needed to make the fiber in close contact with the substances under test, which reduces the reliability of the device. However, in multimode waveguides only a certain number of higher-order modes will be phase matched with a plasmon. Thus, sensitivity and stability of such sensors depend crucially on launch conditions [20].

In recent years, many specialists and scholars put forward photonic crystal fiber (PCF) based SPR sensors. The sensing mechanism is through coupling the leaky core mode to the plasmon to achieve resonance sensing. The use of the photonic crystal fiber, with its flexible design, makes it easy to equate the effective index of the core mode to that of the material under test. Thus phase matching condition between the core mode and the plasmon can be easily achieved at the required wavelength and then resonance occurs. Especially, the fabrication of sensors does not need removing cladding or tapering fibers as traditional fibers do. So there is no problem in the sensor package. Many scientists have put forward a lot of surface plasmon resonance sensor designs based on PCFs and plenty of simulations and calculations have been made, showing great advantages and good application prospects of the new sensors. In 2006, HASSANI and SKOROBOGATIY proposed PCF-based SPR sensors and optimized micro-fluid design concepts, and refractive index resolution of  $10^{-4}$  RIU can be achieved in the structure [21]. In 2008, HAUTAKORPI *et al.* proposed and numerically analyzed a three-hole photonic crystal fiber SPR sensor, with gold film deposited on the inner

wall of the three holes. Numerical results indicate that the optical loss of the Gaussian guided mode can be made very small and that the refractive-index resolution for aqueous analytes is  $1 \times 10^{-4}$  RIU [22].

Metal nanoparticles and nanowires (columns), and other nanostructures can also be used to generate surface plasmon resonance. SPRs at visible wavelengths have been reported in chemically grown gold “nanorods” with diameters of 20 nm [23]. Arrays of parallel nanowires have also been suggested as suitable structures for subwavelength imaging [24].

Surface plasmon resonance sensors based on photonic crystal fiber filled with metal nanowires have not been reported in the literature. In this article, surface plasmon resonance sensors based on photonic crystal fiber filled with silver nanowires have been analyzed through the finite element method (FEM) by using COMSOL Multiphysics software, regularity of the resonant wavelength changing with refractive index of the sample has been numerically simulated, and resonant wavelength detection as well as intensity detection sensitivity have also been discussed. Numerical results show that excellent sensing characteristics of the structure can be achieved as the radius of the silver nanowires is selected in the range of 150 nm to 300 nm, with both spectral and intensity sensitivity in the range of  $4 \times 10^{-5}$ – $5 \times 10^{-5}$  RIU, better than the similar structures coated with metal film. Moreover, the fabrication of these structures needs no coating process.

## **2. SPR sensors based on PCFs filled with silver nanowires of 150 nm radius**

It is very difficult to coat the holes in a photonic crystal fiber with metal film (gold or silver film) of nanometers in thickness of nanoscale, especially for obtaining uniform metal film. In this paper, photonic crystal fiber filled with silver nanowires is considered as an alternative to achieve surface plasmon resonance and the sensing properties of this kind of structure are preliminarily studied. LM-8-type photonic crystal fiber made by NKT Company is used here, with core diameter of 8  $\mu\text{m}$ , cladding air hole diameter of 2.576  $\mu\text{m}$ , and lattice pitch of 5.6  $\mu\text{m}$ .

A photonic crystal fiber selectively filled in the first layer of the holes with silver nanowires of 150 nm radius is first calculated and studied. The fiber and silver nanowires are shown in Fig. 1a. Figure 1b represents the fundamental mode field distribution. Refractive index of the silica glass fiber can be determined by the Sellmeier equation, and the relative permittivity of silver (or refractive index) is taken from an optical handbook [25].

Liquid sample is filled in all the holes and the electromagnetic mode of the sensor fiber is solved with the finite element method (FEM) (optical field distribution of the fundamental mode is shown in Fig. 1b, where the arrow indicates the polarization direction of magnetic field). The attenuation constant of the fundamental mode is

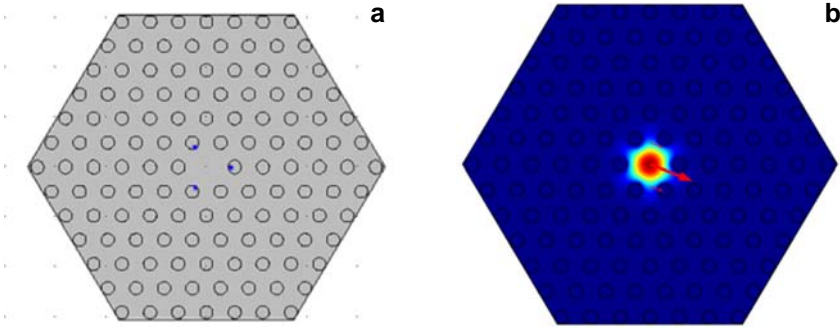


Fig. 1. Structure diagram of the LMA-8 PCF which is partially filled with silver nanowires (indicated by blue dots) of 150 nm radius in the first layer of the holes (a). Optical field distribution of the fundamental mode (b).

calculated for different wavelengths of incident light. The wavelength with maximal transmission loss can be identified and light intensity detection sensitivity at different wavelengths can also be investigated. Assume that the magnetic field solution obtained in optical fiber can be expressed as

$$H(x, y, z) = H(x, y)e^{-i(\beta z - \omega t)} \tag{1}$$

Here,  $\omega$  is the angular frequency of light, and  $t$  denotes time. The propagation constant  $\beta$  can be expressed as

$$\beta = n_{\text{eff}}k_0 \tag{2}$$

where  $k_0 = 2\pi/\lambda$  is the wave number with  $\lambda$  being the free-space wavelength, and  $n_{\text{eff}}$  is the effective index of the mode. The decay in the power of the mode as it propagates through the sensor fiber (toward the positive  $z$ -direction) can be described with the formula

$$P(z) = P_0e^{-\alpha z} \tag{3}$$

where  $P_0$  is the power at the reference plane  $z = 0$ . It is easy to demonstrate that the attenuation constant  $\alpha$  is proportional to the imaginary part of the effective index, and

$$\alpha = 2k_0 \text{Im}(n_{\text{eff}}) \tag{4}$$

In fact, fiber transmission loss coefficient is defined as

$$\alpha_{\text{loss}} = \frac{10}{Z} \log\left(\frac{P_0}{P(z)}\right) \tag{5}$$

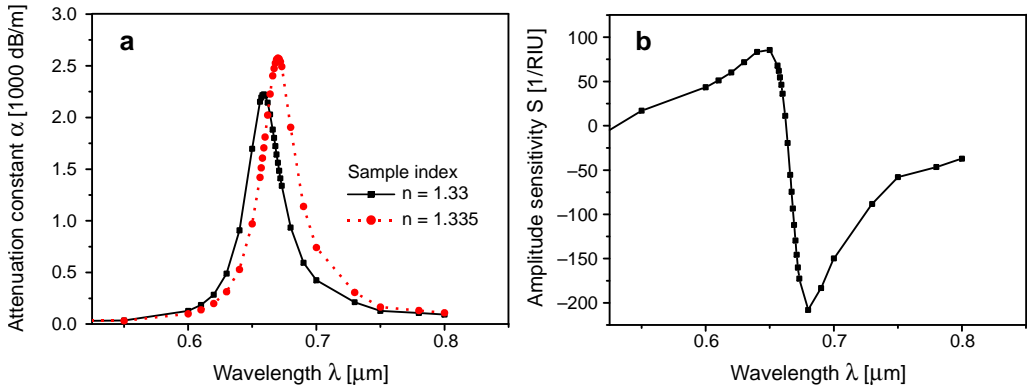


Fig. 2. Relationship between wavelength and attenuation constant of the fundamental mode of the LMA-8 PCF with the first layer of the holes partially filled with silver nanowires of 150 nm radius (a). Intensity detection sensitivity curve (b).

From the above two equations,  $\alpha_{\text{loss}} = 10\log(e)\alpha = 4.343\alpha$  can be obtained. As can be seen, there is only a constant factor difference. For ease of understanding and convenience, the power attenuation constant  $\alpha$  is used to quantify the loss of the mode, and dB/m is still used as the unit.

For the first layer of the holes of the LMA-8 PCF being partially filled with silver nanowires of 150 nm radius, the relationship between wavelength and attenuation constant of the fundamental mode is shown in Fig. 2a, in which the solid and dotted curves represent the refractive indices of the samples, which are 1.33 and 1.335, respectively. As shown in the figure, there is a sharp loss peak in the range of 600–700 nm for each curve. That is because the resonance between the core mode and the surface plasmon makes great energy loss of light field in the core. When the refractive index of the sample changes from 1.33 to 1.335 ( $\Delta n_a = 0.005$ ), the resonance peak shifts toward longer wavelength, and the amount of shift is about 11 nm ( $\Delta\lambda_{\text{peak}}$ ). If the instrumental peak-wavelength resolution is assumed to be  $\Delta\lambda_{\text{min}} = 0.1$  nm, the refractive index resolution of the corresponding sensor can be obtained as

$$R = \Delta n_a \frac{\Delta\lambda_{\text{min}}}{\Delta\lambda_{\text{peak}}} = 4.55 \times 10^{-5} \text{ RIU} \tag{6}$$

Another detection method is known as the power detection at a fixed single wavelength, which is also known as amplitude based detection method. Assume that the wavelength of the light is  $\lambda$ , and the transmission length is  $L$ , and then the power detection sensitivity for the refractive index variation  $\Delta n_a$  can be defined as

$$S(\lambda) = \frac{P(L, \lambda, n_a + \Delta n_a) - P(L, \lambda, n_a)}{P(L, \lambda, n_a) / (\Delta n_a)} \tag{7}$$

The sensor length  $L$  is typically limited by the modal transmission loss. A reasonable choice of a sensor length is  $L = 1/\alpha(\lambda, n_a)$ . Such choice of a sensor length results in a simple definition of sensitivity for the small changes in the analyte refractive index [26]

$$S(\lambda) = \frac{1}{P(L, \lambda, n_a)} \frac{\partial P(L, \lambda, n_a)}{\partial n_a} = \frac{1}{\alpha(\lambda, n_a)} \frac{\partial \alpha(\lambda, n_a)}{\partial n_a} \quad (8)$$

In Figure 2b we present the amplitude sensitivity curve of the computed PCF-based SPR sensor filled with silver nanowires of 150 nm radius. As can be seen in the diagram, the maximal sensitivity is achieved at 680 nm and equals  $208 \text{ RIU}^{-1}$ . It is typically a safe assumption that a 1% change in the transmitted intensity can be detected reliably, which leads to the sensor resolution of  $4.8 \times 10^{-5} \text{ RIU}$ .

### 3. SPR sensors based on PCFs filled with silver nanowires of 50 nm and 300 nm radii

For the radius of silver nanowires changing to 50 nm, attenuation spectrum of the fundamental mode and the amplitude detection sensitivity curve are shown in Fig. 3a and 3b, respectively. As shown in Fig. 3a, there are two close-set resonance peaks and both of them are not sharp enough and not sensitive to the variation of the sample refractive index. Amplitude detection sensitivity is not high enough, either. In our opinion, there is a degenerate SPW mode around the silver nanowires. If the nanowires are large enough, the evanescent waves inside the silver nanowires do not overlap. As the nanowire thickness decreases, the evanescent waves of the otherwise decoupled modes begin to overlap, and the degenerate SPW mode therefore splits into two different modes.

When the radius of silver nanowires increases to 300 nm, the corresponding fundamental mode attenuation spectrum and amplitude detection sensitivity curve can

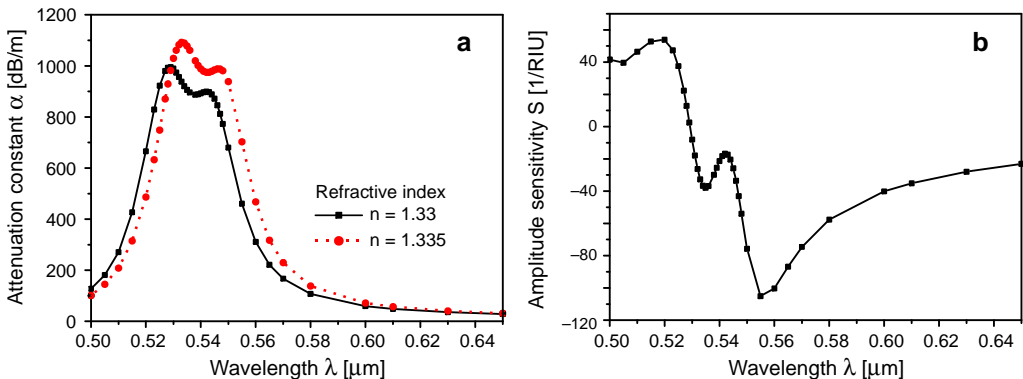


Fig. 3. Relationship between wavelength and attenuation constant of fundamental mode of the LMA-8 PCF with the first layer of the holes partially filled with silver nanowires of 50 nm radius (a). Intensity detection sensitivity curve (b).

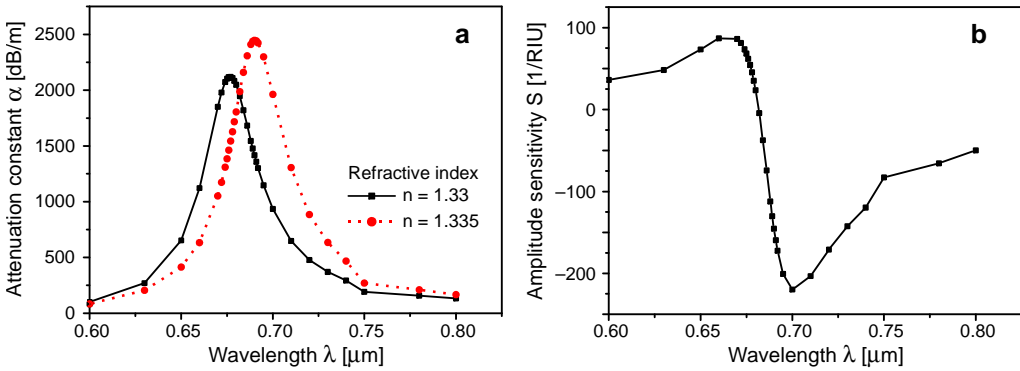


Fig. 4. Relationship between wavelength and attenuation constant of fundamental mode of the LMA-8 PCF with the first layer of the holes partially filled with silver nanowires of 50 nm radius (a). Intensity detection sensitivity curve (b).

be obtained, as shown in Figs. 4a and 4b, respectively. When the refractive index of the sample changes from 1.33 to 1.335 ( $\Delta n_a = 0.005$ ), the resonance peak shifts toward longer wavelength, and 13 nm of red shift ( $\Delta \lambda_{\text{peak}}$ ) can be achieved, corresponding to the spectral resolution of refractive index of  $3.85 \times 10^{-5}$  RIU. The maximal amplitude sensitivity is achieved at 700 nm and equals  $220 \text{ RIU}^{-1}$ . It is also assumed that a 1% change in the transmitted intensity can be detected reliably, leading to the sensor resolution of  $4.8 \times 10^{-5}$  RIU. A slight improvement is achieved compared with the radius of 150 nm.

After several calculations, the relationship between the refractive index resolution of spectral detection and the radius of silver nanowires is shown in Fig. 5. In the diagram, we can see the refractive index resolution is improved as the radius of silver nanowires increases within the radius range of 100–300 nm. For larger size of nanowires, the index resolution is no longer improved, or even decreased.

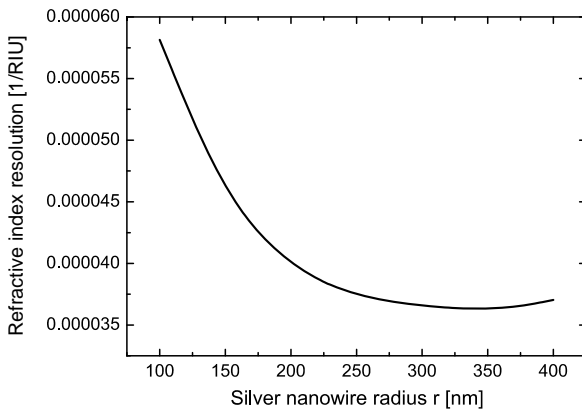


Fig. 5. Relationship between the refractive index resolution of spectral detection and the radius of silver nanowires.

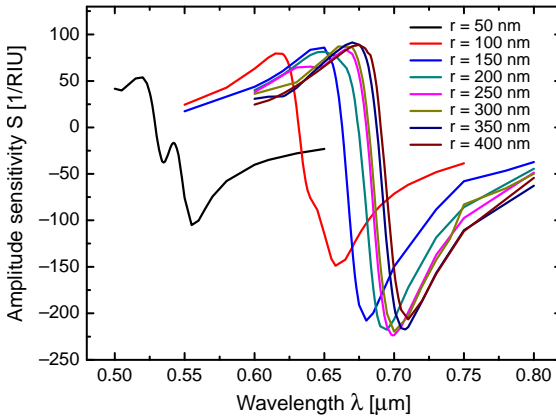


Fig. 6. Intensity detection sensitivity curve corresponding to the PCF filled with different sizes of silver nanowires.

Intensity detection sensitivity curve corresponding to the PCF filled with different sizes of silver nanowires is plotted in Fig. 6. The maximal amplitude sensitivity also increases as the radius of silver nanowires increases, and starts to decrease down to a certain range, which is similar to the resolution of spectral detection.

#### 4. SPR sensors based on PCFs filled with silver nanowires of 150 nm radius in the second layer of holes

From the contents mentioned above, we can see that fiber loss is quite large with silver nanowires filled in the first layer of the holes, which greatly limits the length of the sensing fiber (less than 1 mm). In order to reduce the transmission loss, silver nanowires are selectively filled in the second layer of holes, which is shown in Fig. 7a. Figure 7b represents the fundamental mode field distribution.

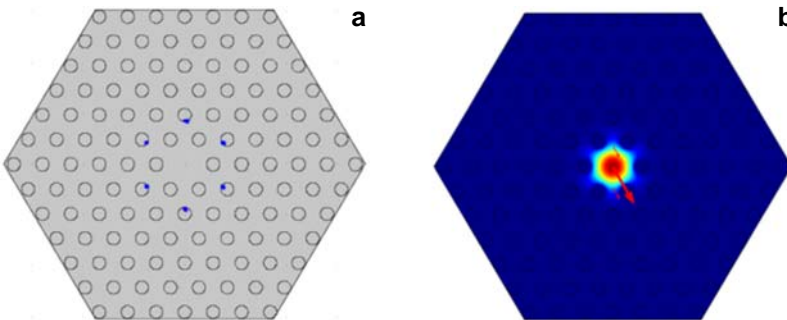


Fig. 7. Structure diagram of the LMA-8 PCF which is partially filled with silver nanowires (indicated by blue dots) of 150 nm radius in the second layer of the holes (a). Optical field distribution of fundamental mode (b).

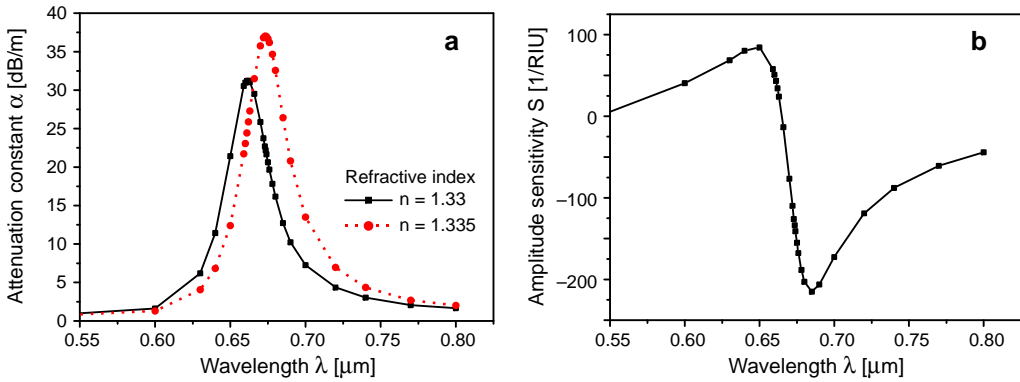


Fig. 8. Relationship between wavelength and attenuation constant of fundamental mode of the LMA-8 PCF with the second layer of the holes partially filled with silver nanowires of 50 nm radius (a). Intensity detection sensitivity curve (b).

The relationship between wavelength  $\lambda$  and attenuation constant of the fundamental mode  $\alpha$  is shown in Fig. 8a, in which the solid and dotted curves represent the refractive indices of the samples, which are 1.33 and 1.335, respectively. When the refractive index of the sample changes from 1.33 to 1.335 ( $\Delta n_a = 0.005$ ), 11 nm of red shift ( $\Delta \lambda_{\text{peak}}$ ) of the resonance peak can be achieved, corresponding to the spectral detection resolution of  $4.55 \times 10^{-5}$  RIU. The maximal amplitude sensitivity is achieved at 680 nm and equals  $203 \text{ RIU}^{-1}$ . It is also assumed that a 1% change in the transmitted intensity can be detected reliably leading to the sensor resolution of  $4.9 \times 10^{-5}$  RIU. It is clear that the fiber loss is largely reduced, as the silver nanowires are filled in the second layer of holes, and the sensor can reach an order of magnitude of 2–3 cm in length, while maintaining similar  $\lambda$  sensitivity.

## 5. Summary

Surface plasmon resonance sensors based on photonic crystal fibers filled with silver nanowires of different sizes have been analyzed through the finite element method (FEM) by using COMSOL Multiphysics software and the sensing properties are discussed in both areas of resonant wavelength and intensity detection. Numerical results show that excellent sensing characteristics of the structure can be achieved as the radius of the silver nanowires is selected in the range from 150 to 300 nm, with both spectral and intensity sensitivity in the range of  $4 \times 10^{-5}$ – $5 \times 10^{-5}$  RIU. Moreover, the fabrication of these sensor structures needs no coating process.

It is also found that the sensors with silver nanowires filled in the second layer of holes can reach 2–3 cm in length, while having high sensing sensitivity

*Acknowledgements* – The authors would like to thank the support of Major State Basic Research Development Program of China (973 Program) (grant number: 2010CB327801) and the National Natural Science Foundation of China (grant number: 10874128) for the work reported in this paper.

## References

- [1] BYOUNGHO LEE, SOOKYOUNG ROH, JUNGHYUN PARK, *Current status of micro- and nano-structured optical fiber sensors*, *Optical Fiber Technology* **15**(3), 2009, pp. 209–221.
- [2] SHARMA A.K., JHA R., GUPTA B.D., *Fiber-optic sensors based on surface plasmon resonance: A comprehensive review*, *IEEE Sensors Journal* **7**(8), 2007, pp. 1118–1129.
- [3] OTTO A., *Excitation of nonradiative surface plasma waves in silver by the method of frustrated total reflection*, *Zeitschrift für Physik A* **216**(4), 1968, pp. 398–410.
- [4] KRETSCHMANN E., REATHER H., *Radiative decay of non-radiative surface plasmons excited by light*, *Zeitschrift für Naturforschung* **23**, 1968, pp. 2135–2136.
- [5] KRETSCHMANN E., *Die Bestimmung optischer Konstanten von Metallen durch Anregung von Oberflächenplasmaschwingungen*, *Zeitschrift für Physik A* **241**(4), 1971, pp. 313–324.
- [6] LIEDBERG B., NYLANDER C., LUNDSTRÖM I., *Surface plasmon resonance for gas detection and biosensing*, *Sensors and Actuators* **4**, 1983, pp. 299–304.
- [7] MELENDEZA J., CARRA R., BARTHOLOMEWA D.U., KUKANSKIS K., ELKIND J., YEE S., FURLONG C., WOODBURY R., *A commercial solution for surface plasmon sensing*, *Sensors and Actuators B* **35**(1–3), 1996, pp. 212–216.
- [8] ZHANG L.M., UTTAMCHANDANI D., *Optical chemical sensing employing surface plasmon resonance*, *Electronics Letters* **24**(23), 1988, pp. 1469–1470.
- [9] KABASHIN A.V., NIKITIN P.I., *Surface plasmon resonance interferometer for bio- and chemical-sensors*, *Optics Communications* **150**(1–6), 1998, pp. 5–8.
- [10] GRIGORENKO A.N., NIKITIN P.I., KABASHIN A.V., *Phase jumps and interferometric surface plasmon resonance imaging*, *Applied Physics Letters* **75**(25), 1999, pp. 3917–3919.
- [11] MANUEL M., VIDAL B., LÓPEZ R., ALEGRET S., ALONSO-CHAMARRO J., GARCES I., MATEO J., *Determination of probable alcohol yield in musts by means of an SPR optical sensor*, *Sensors and Actuators B* **11**(1–3), 1993, pp. 455–459.
- [12] ALONSO R., SUBÍAS J., PELAYO J., VILLUENDAS F., TORNOS J., *Single-mode, optical-fiber sensors and tunable wavelength filters based on the resonant excitation of metal-clad modes*, *Applied Optics* **33**(22), 1994, pp. 5197–5201.
- [13] HOMOLA J., *Optical fiber sensor based on surface plasmon resonance excitation*, *Sensors and Actuators B* **29**(1–3), 1995, pp. 401–405.
- [14] TUBB A.J.C., PAYNE F.P., MILLINGTON R.B., LOWE C.R., *Single-mode optical fibre surface plasma wave chemical sensor*, *Sensors and Actuators B* **41**(1–3), 1997, pp. 71–79.
- [15] DíEZ A., ANDRÉS M.V., CRUZ J.L., *In-line fiber-optic sensors based on the excitation of surface plasma modes in metal-coated tapered fibers*, *Sensors and Actuators B* **73**(2–3), 2001, pp. 95–99.
- [16] PILIARIK M., HOMOLA J., MANÍKOVA Z., ČTYROKÝ J., *Surface plasmon resonance sensor based on a single-mode polarization-maintaining optical fiber*, *Sensors and Actuators B* **90**(1–3), 2003, pp. 236–242.
- [17] MONZON-HERNANDEZ D., VILLATORO J., TALAVERA D., LUNA-MORENO D., *Optical-fiber surface-plasmon resonance sensor with multiple resonance peaks*, *Applied Optics* **43**(6), 2004, pp. 1216–1220.
- [18] GUPTA B.D., SHARMA A.K., *Sensitivity evaluation of a multi-layered surface plasmon resonance-based fiber optic sensor: A theoretical study*, *Sensors and Actuators B* **107**(1), 2005, pp. 40–46.
- [19] MONZÓN-HERNANDEZ D., VILLATORO J., *High-resolution refractive index sensing by means of a multiple-peak surface plasmon resonance optical fiber sensor*, *Sensors and Actuators B* **115**(1), 2006, pp. 227–231.
- [20] HASSANI A., GAUVREAU B., FASSI FEHRI M., KABASHIN A., SKOROBOGATIY M., *Photonic crystal fiber and waveguide-based surface plasmon resonance sensors for application in the visible and near-IR*, *Electromagnetics* **28**(3), 2008, pp. 198–213.
- [21] HASSANI A., SKOROBOGATIY M., *Design of the microstructured optical fiber-based surface plasmon resonance sensors with enhanced microfluidics*, *Optics Express* **14**(24), 2006, pp. 11616–11621.

- [22] HAUTAKORPI M., MATTINEN M., LUDVIGSEN H., *Surface-plasmon-resonance sensor based on three-hole microstructured optical fiber*, Optics Express **16**(12), 2008, pp. 8427–8432.
- [23] PELTON M., MINGZHAO LIU, SUNGNAM PARK, SCHERER N.F., GUYOT-SIONNEST P., *Ultrafast resonant optical scattering from single gold nanorods: Large nonlinearities and plasmon saturation*, Physical Review B **73**(15), 2006, p. 155419.
- [24] ELSEER J., WANGBERG R., PODOLSKIY V.A., NARIMANOV E.E., *Nanowire metamaterials with extreme optical anisotropy*, Applied Physics Letters **89**(26), 2006, p. 261102.
- [25] PALIK E.D., *Handbook of Optical Constants of Solids*, Academic Press, Boston, 1985.
- [26] GAUVREAU B., HASSANI A., FASSI FEHRI M., KABASHIN A., SKOROBOGATIIY M.A., *Photonic bandgap fiber-based surface plasmon resonance sensors*, Optics Express **15**(18), 2007, pp. 11413–11426.

*Received April 23, 2011  
in revised form May 27, 2011*